

# **Biogenic Aerosols – Effects on Climate and Clouds: Cloud Optical Depth (COD) Sensor Three-Waveband Spectrally-Agile Technique (TWST) Field Campaign Report**

ER Niple  
HE Scott

April 2016

## **DISCLAIMER**

This report was prepared as an account of work sponsored by the U.S. Government. Neither the United States nor any agency thereof, nor any of their employees, makes any warranty, express or implied, or assumes any legal liability or responsibility for the accuracy, completeness, or usefulness of any information, apparatus, product, or process disclosed, or represents that its use would not infringe privately owned rights. Reference herein to any specific commercial product, process, or service by trade name, trademark, manufacturer, or otherwise, does not necessarily constitute or imply its endorsement, recommendation, or favoring by the U.S. Government or any agency thereof. The views and opinions of authors expressed herein do not necessarily state or reflect those of the U.S. Government or any agency thereof.

**Biogenic Aerosols – Effects on Climate  
and Clouds: Cloud Optical Depth (COD)  
Sensor Three-Waveband Spectrally-  
Agile Technique (TWST)  
Field Campaign Report**

ER Niple, Aerodyne Research, Inc.  
HE Scott, Aerodyne Research, Inc.  
Principal Investigators

April 2016

Work supported by the U.S. Department of Energy,  
Office of Science, Office of Biological and Environmental Research

## **Acknowledgments**

We gratefully acknowledge the assistance of Niki Hickmon, ARM Southern Great Plains (SGP)/second ARM Mobile Facility (AMF2) Site Manager, Michael T. Ritsche, and Deborah Busch, all at Argonne National Laboratory. We owe a special thanks to the Biogenic Aerosols Effects on Climate and Clouds (BAECC) onsite staff in Finland who were quite skilled and gave attention to every detail in our instructions.

This work was supported by the U.S. Department of Energy (DOE)'s Atmospheric Radiation Measurement (ARM) Climate Research Facility, Atmospheric Sciences and Global Change Division, Pacific Northwest National Laboratory, P.O. 236318.

## Acronyms and Abbreviations

AERONET	Aerosol Robotic Network
AOD	aerosol optical depth
AMF2	second ARM Mobile Facility
ARM	Atmospheric Radiation Measurement Climate Research Facility
BAECC	Biogenic Aerosols Effects on Climate and Clouds
cm	centimeter
COD	Cloud Optical Depth
1D	one-dimensional
3D	three-dimensional
DISORT	discrete ordinate radiative transfer
DOE	U.S. Department of Energy
Hz	hertz
IP	Internet Protocol
Km	kilometer
msec	millisecond
OD	optical depth
nm	nanometer
SNR	signal-to-noise ratio
TCAP	Two-Column Aerosol Project
TSI	Total Sky Imager
TWST	Three-Waveband Spectrally-Agile Technique
UPS	uninterruptible power supply
USB	Universal Serial Bus
UTC	Coordinated Universal Time

## Contents

Acknowledgments.....	iii
Acronyms and Abbreviations .....	iv
1.0 Overview .....	1
2.0 TWST Theory of Operation .....	1
3.0 TWST Deployment.....	2
4.0 TWST Data Catalog .....	3
5.0 TWST Results.....	5
5.1 General Comments on Results .....	7
5.1.1 Absolute Accuracy and Relative Precision of the TWST COD Measurements.....	7
5.1.2 Limitations of the Data.....	7
5.2 Specific Comments on Results.....	8
5.2.1 Frequently Cloud-free Conditions Analysis, July 23-25 .....	8
6.0 TWST ARM Data Archive Description .....	13
7.0 Bibliography.....	14
Appendix A Daily Summary Plots.....	A.1

## Figures

1. TWST optical head as deployed during BAECC.....	2
2. TWST sensor location, shown here on the tripod in the foreground, in relation to other cloud and aerosol sensors during BAECC campaign .....	3
3. Calendar for July 2014 showing the days when TWST data were collected.....	4
4. Calendar for August 2014 showing the days when TWST data were collected.....	5
5. Sample of Daily Summary data from Appendix A.....	6
6. Spectral Radiance at 440 nm for 23-25 July 2014 plotted against Solar Zenith Angle.....	9
7. Spectral Radiance at 870 nm for 23-25 July 2014 plotted against Solar Zenith Angle.....	9
8. Spectral Radiance at 440 nm for 23-25 July 2014 plotted against Solar Zenith Angle overlaid with the expected spectral radiance at 440 nm for four levels of aerosol.....	10
9. Spectral Radiance at 870 nm for 23-25 July 2014 plotted against Solar Zenith Angle overlaid with the expected spectral radiance at 870 nm for four levels of aerosol.....	11
10. Spectral Radiance at 440 and 870 nm and the equivalent width of the oxygen A-band versus time. ....	12
11. Cloud shadow from TSI sensor for July 24 2014 9:39 UTC.....	13

## 1.0 Overview

This report describes the data collected by the Three-Waveband Spectrally-agile Technique (TWST) sensor deployed at Hyytiälä, Finland from 16 July to 31 August 2014 as a guest on the Biogenic Aerosols Effects on Climate and Clouds (BAECC) campaign. These data are currently available from the Atmospheric Radiation Measurement (ARM) Data Archive website and consists of Cloud Optical Depth (COD) measurements for the clouds directly overhead approximately every second (with some dropouts described below) during the daylight periods. A good range of cloud conditions were observed from clear sky to heavy rainfall.

## 2.0 TWST Theory of Operation

The TWST sensor directly collects calibrated spectral radiance at zenith for the spectral range of 350-1000 nanometers (nm) at ~2 nm spectral resolution. In standalone mode, it retrieves COD at a sample rate of 1 hertz (Hz) using the spectral radiance at 440 nm and the equivalent width of the oxygen A-band at 760 nm. TWST participated in the ARM Two-Column Aerosol Project (TCAP) campaign on Cape Cod, Massachusetts, in June 2013. The Aerodyne TCAP report (Niple 2013) includes comparisons of TWST and the Aerosol Robotic Network (AERONET) (Holben 1998) Cloud Mode (Chiu and Chiung-Huei Huang 2010) results.

The TWST sensor consists of two main components: the optical head and the data collection/control computer. The optical head (Figure 1) is mounted on a tripod and connected to the computer by a 50-foot Universal Serial Bus (USB) cable that provides both power and communication functions. The heart of the TWST optical head is a compact grating spectrometer. This is connected through an optical fiber to a collimating lens and sun baffle. A mechanical shutter is located in the collimated exit beam for dark spectrum collection. All the optical components are located in a sealed enclosure, with a separately sealed sun baffle extension mounted on the enclosure.



**Figure 1.** TWST optical head as deployed during BAECC.

The raw TWST data is an uncalibrated set of counts for each of 2048 spectral channels that is stored on the computer. These are then calibrated and reduced to produce the COD during post-processing. A preliminary real-time COD is also displayed by the TWST data-logging software for onsite monitoring purposes. For the BAECC campaign, TWST uploaded the raw data to a special Dropbox® account. In addition, the TeamViewer® software application was used for real-time control of the sensor, if needed.

The data processing algorithm starts with the calibrated zenith spectral radiance at 440 and 870 nm wavelengths plus the equivalent width of the oxygen A-band near 760 nm for each one-second time period. The ratio of the 440 and 870 spectral radiances and the equivalent width are then run through a nonlinear filter to estimate the optical state (i.e., optically thick or optically thin) of the cloud overhead. The optical state is then used to select which of two pre-computed 440 nm spectral radiance lookup tables is used to identify the corresponding COD. The tables are computed using the MODTRAN® 5.2 (Berk 2011) computer model. MODTRAN® is the “U.S. Air Force standard moderate spectral resolution radiative transport model”. It includes the DISORT (discrete ordinate radiative transfer) module for multiple scattering within clouds and aerosols. The coordinated universal time (UTC) of the observation and the location (longitude and latitude) of the sensor are used to compute the solar zenith angle for each measurement, which in turn is used to interpolate the proper row of the pre-computed tables.

### 3.0 TWST Deployment

The TWST sensor was deployed in close proximity to other sensors (Figure 2) useful for joint analysis of both cloud and aerosol measurement. These other sensors consist of the Total Sky Imager (TSI), the AERONET sensor, scanning and fixed cloud radar, and microwave radiometers. The control computer was located inside the white seatainer shown behind and to the left of the optical head.



**Figure 2.** TWST sensor location, shown here on the tripod in the foreground, in relation to other cloud and aerosol sensors during BAECC campaign. The Cimel sun photometer used for the AERONET sensor is indicated in the figure by a red arrow. The TWST computer is located in the white seatainer behind and to the left of the TWST optical head.

The power needed by the TWST optical head is supplied by the same USB cable that provides communication. The control computer was a Getac B300 ultra-rugged notebook with a four-hour battery life. This computer provided some protection from brief site power interruptions (20 July) and long power interruptions (July 26 and 31), but it caused some TWST data loss. Restoring TWST after such an outage required onsite personnel to restart the computer and launch the control software. In addition, we suspect a power spike during the July 31 lightning strike as the most probable reason for the data loss on that day. The onsite staff recommended that the control computer be plugged into an uninterruptible power supply (UPS) to provide power regulation as well as backup power during outages. After this change was made, and the power supply network was re-configured, no further data loss occurred.

An Internet Protocol (IP) address and Gigabit Ethernet connection was assigned to the TWST control computer to assist with our data storage. This provided a fast uplink capability to the Dropbox® account used to store raw TWST data prior to post-processing. This was also used to remotely control the computer with the TeamViewer® software when needed for trouble-shooting. We only needed to use this capability once on July 22 to adjust a detector threshold to avoid excess baseline drift. As with recovery from a long power outage, onsite personnel were required to launch the TeamViewer® application on the control computer before remote operation could be established. Because of our direct connection to the Internet, virus software protection was installed and frequent virus scans were scheduled at night.

## 4.0 TWST Data Catalog

TWST was deployed on 16 July 2014 and began data collection at 13:00 UTC. The daily conditions and data logs (Figure 3 and Figure 4) show the overall set of TWST COD data collected during BAECC. After an initial period of 10 days with occasional data loss, TWST then operated for 36 days without

interruption or need for further adjustment. It was taken down and packed for return shipment on August 31. The total number of COD values collected by TWST during the BAECC campaign was 2,333,457.

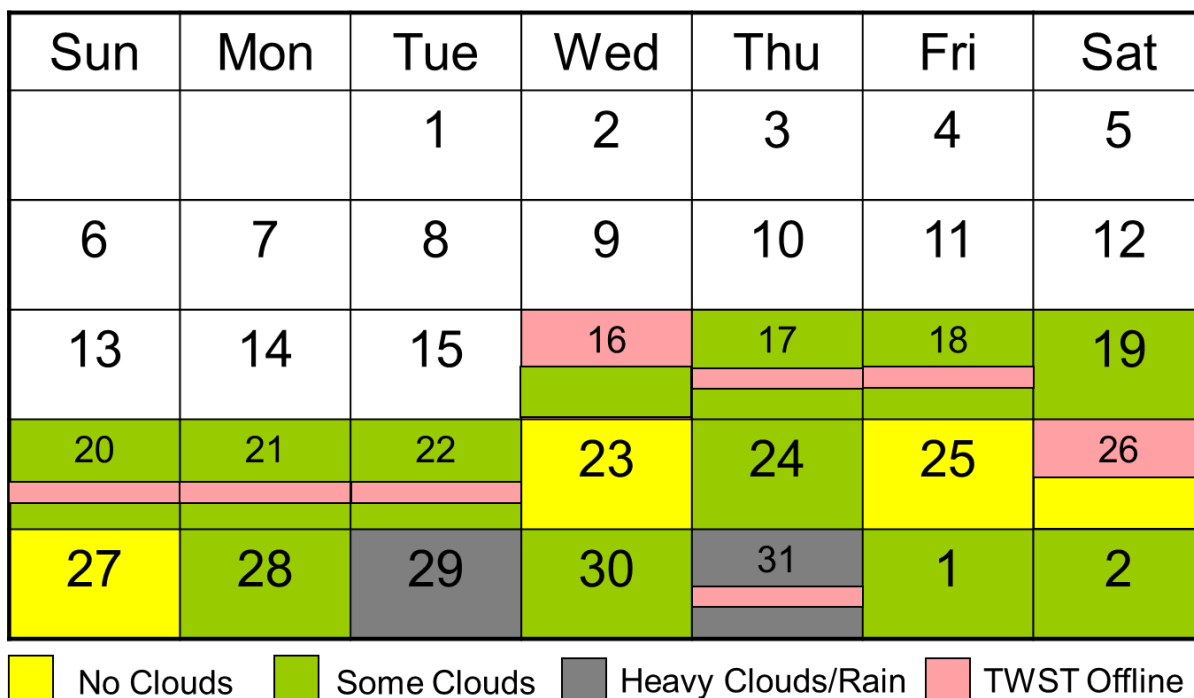


**Figure 3.** Calendar for July 2014 showing the days when TWST data were collected. The approximate cloud conditions are indicated by the color scheme shown in the legend. The offline period during 16 July was during the initial setup of TWST by onsite personnel. The offline periods on 26 and 31 July were caused by major power outages. The offline periods from 17 to 22 July were due to baseline drift as a result of very hot conditions during the day. This was corrected on 22 July.

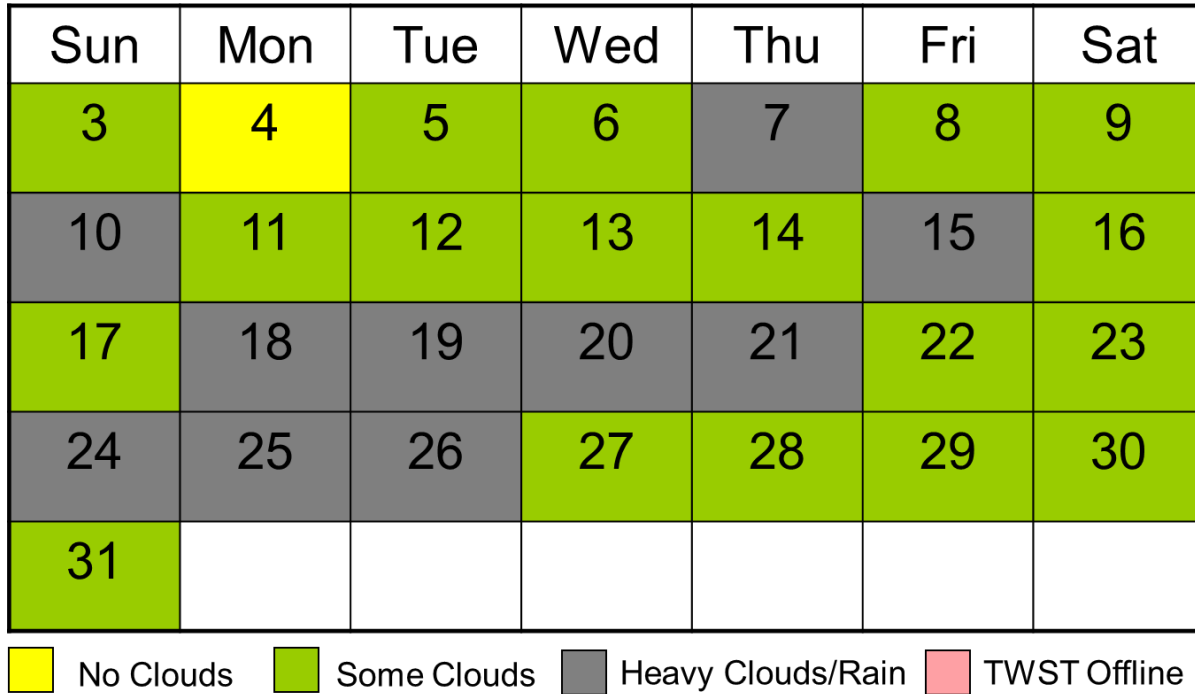


**Figure 4.** Calendar for August 2014 showing the days when TWST data were collected. The approximate cloud conditions are indicated by the color scheme shown in the legend. TWST was taken down on August 31.

## 5.0 TWST Results

For each of the days that TWST was deployed in Finland, we have prepared two summary charts that show the inputs and the outputs from the post-processing. These are included in Appendix A. A sample is given below (Figure 5). The first of the two plots shows the calibrated spectral radiances at 440 (blue line) and 870 (orange line) nm (in units of microwatts/cm<sup>2</sup> sr nm) along with the equivalent width (gray line) of the oxygen A-band (in units of nm) for the entire daylight period. The second plot shows the corresponding optically thin (blue line) and optically thick (orange line) CODs and the post-processing algorithm’s selection (gray squares) for the final COD based on the estimated cloud state (optically thick or optically thin). These final COD values are labelled “RatCOD” in the plot legends.

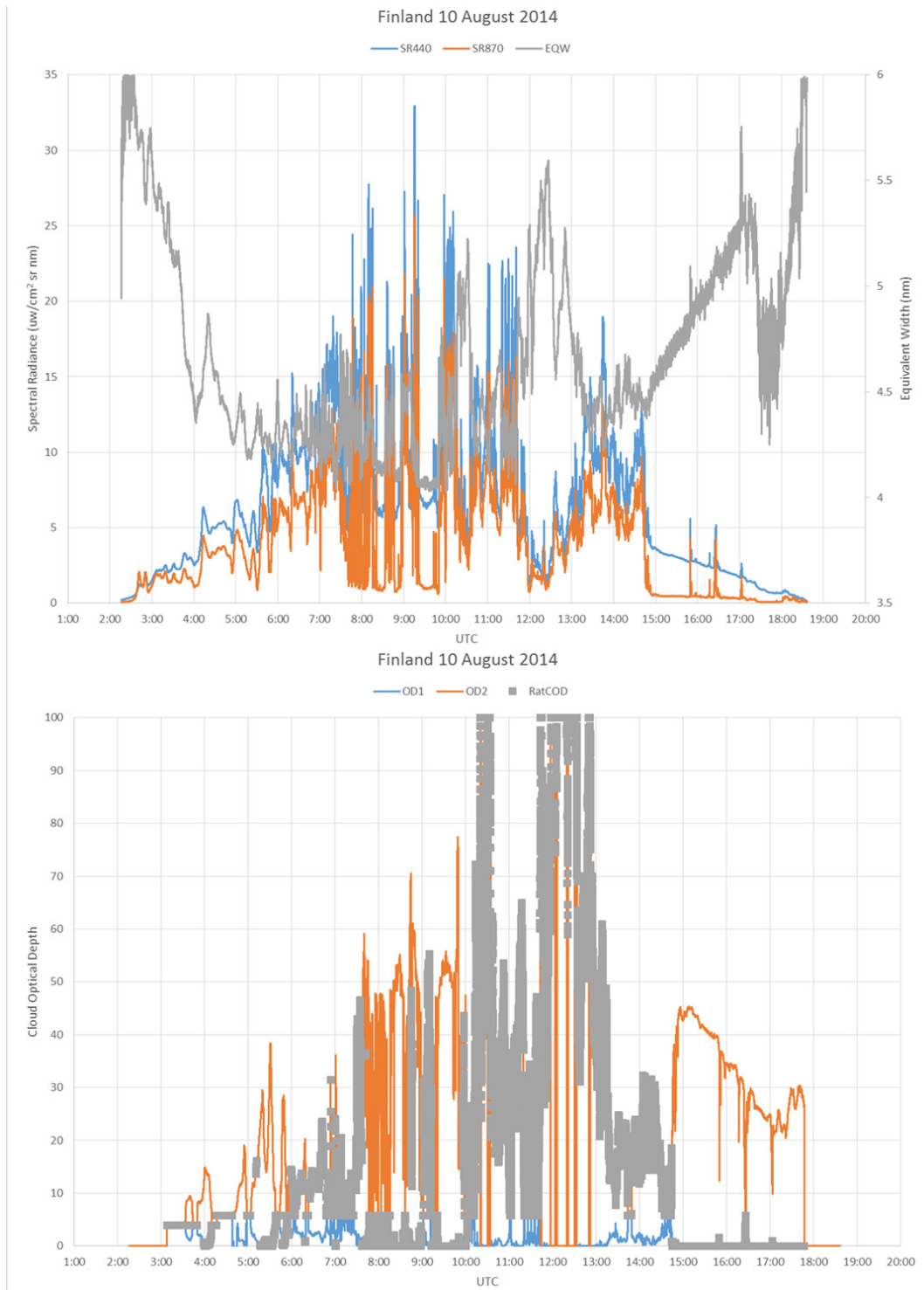


**Figure 5.** Sample of Daily Summary data from Appendix A. This is the data for 10 August 2014 showing, in the top plot, the inputs to the COD algorithm: spectral radiance at 440 (blue line) and 870 (orange line) nm wavelengths and equivalent width of the oxygen A-band (gray line), and, in the bottom plot, the cloud optical depths for optically thin (blue line) and optically thick (orange line) cloud states and the value selected by our COD algorithm (gray squares) based on the estimated cloud state.

## 5.1 General Comments on Results

Before discussing individual results, we have a few general comments.

### 5.1.1 Absolute Accuracy and Relative Precision of the TWST COD Measurements

Each raw TWST spectrum consists of 400 co-added scans of 2.5 millisecond (msec) integration time. The signal-to-noise ratio (SNR) for a single scan is limited to 400:1 due to photon noise based on the electron well depth of 160,000 photons. When readout noise is included, this drops to 275:1. With 400 co-adds, the 1-second SNR is therefore limited to 5,500:1. This is the relative precision of our reported results. Even higher precision could be achieved by combining the 137 independent spectral channels in the 425-475 nm spectral band. This yields a potential SNR of 64,000:1 for each 1-second spectral radiance value. In terms of COD SNR, for the optically thin state, the COD runs from 0 to about 6 in an approximately linear relationship. This implies a theoretical noise-limited sensitivity of  $6/64,000 = \text{OD (optical depth) } 0.0001$ . Given that Aerosol Optical Depths (AOD) range from OD 0 to 0.5, TWST is easily able to characterize total column AOD, provided that the cloud and aerosol contributions can be separated.

An even higher precision can be achieved by combining multiple one-second time bins for the duration of a cloud/aerosol event. For real-world clouds, we have found a duration of one second or less to be typical, no doubt a combination of cloud drift in the mean wind in addition to cloud evolution. For cloud-free conditions, however, much longer stable periods can exist.

The absolute accuracy of the TWST COD values is probably no better than 5%, which is the estimated accuracy of our radiometric calibration procedure. By measuring the responsivity both before and after each test, we have determined that TWST has an excellent radiometric stability, on the order of a few percent, which is limited by the stability of the lamp used in our LabSphere URS-600 uniform radiance standard. This includes any alignment changes during shipping and deployment as well as drift during the field test. One potentially large source of drift during a field test is buildup of dust on the TWST window. This was minimized during the BAEECC campaign by daily window cleaning, usually in the early morning, by onsite personnel. This created brief artifacts in the COD data that were not removed from the data presented here.

### 5.1.2 Limitations of the Data

The COD algorithm imposes an upper limit of OD 100 on the derived values because of the difficulty of computing the corresponding radiances with MODTRAN®. Often this coincides with heavy rain that causes water drops to form on the slanted TWST window. These drops become part of the COD determined by the algorithm, biasing the final COD. In addition, our algorithm imposes an upper limit of 6 nm on the measured equivalent width. This provides further screening-out of questionable COD measurements.

Any periods of data loss during a day are indicated by blue bands overlaid on the plots and labelled with the cause of the loss (“Baseline Drift” or “Power Loss”). When either the beginning or end of the day are lost, no blue bands are shown. This only occurred from late on July 25 until about mid-day on July 26.

Because our technique relies on scattered sunlight, times when the sun is close to the horizon involve long lines of sight running nearly parallel to the cloud deck. With ideal plane-parallel cloud layers, this presents no problems, but with real-world clouds these long lines of sight often interact with the spatial structure of the cloud tops, leading to erroneous derived COD values.

A more general limitation of TWST is that caused by the assumption of plane-parallel cloud layers in the lookup tables. This limitation is shared by all radiance-based techniques. Techniques that rely on measured fluxes, however, are even more limited by this one-dimensional (1D) cloud assumption. Radiance techniques assume 1D cloud conditions over only the small portion of the cloud around their narrow (0.5 degree) line of sight.

Another limitation caused by the lookup tables is the assumption of minimal variation with cloud base altitude and cloud type. This has been investigated for a range of common cloud types (Conant 2014), and can cause modest errors (5-10%) in derived COD values. When combined with information from other sensors, this potential limitation can be minimized at the expense of creating custom lookup tables that include these effects.

As with all previous TWST field campaigns, in this report we have not attempted to derive AOD for cloudless situations, although this can be done using good all-sky imagery. An example of this is discussed under the specific results section below. For those times when our algorithm would return very small COD values (less than OD 0.1), the algorithm assigns default optical depth values of 0.01 for blue sky situations and 0.02 for slightly higher optical depth situations. These correspond to low values of the 440 nm spectral radiance, below the minimum value listed in the lookup tables. The blue sky state corresponds to a ratio of 440 nm spectral radiance to 870 nm spectral radiance greater than 4. The slightly higher case (the bluish state) corresponds to ratios between 2 and 4.

## 5.2 Specific Comments on Results

### 5.2.1 Frequently Cloud-free Conditions Analysis, July 23-25

During the July 23-25 period, frequently cloud-free conditions existed. In preparation for a more detailed analysis of our TWST data for aerosol-dominated effects, we conducted a preliminary analysis. As shown in the daily summary plots for these three days in Appendix A, the equivalent width curve (gray line on left-hand summary plot) shows a nearly U-shaped behavior during the day with a few brief spikes, usually around mid-day. These spikes are caused by isolated clouds passing overhead. The noisy nature of the gray curve is indicative of clear sky conditions when the spectral radiance in the 760 nm spectral region is very weak, being dominated by Rayleigh scattering by air molecules. Also the very brief spikes early in the morning (around 5:00 UTC) when the TWST window was being cleaned are evident on these plots.

Since the intensity of Rayleigh scatter basically depends only on the solar zenith angle, it is interesting to plot the daily spectral radiances versus solar zenith angle instead of time of day. For cloud- and aerosol-free conditions, this would produce two line segments, one for the morning and one for the afternoon, that lie on top of each other. Any overlap errors are clear evidence of aerosol and cloud effects. As the air temperature warms up during the day, the aerosol scattering often increases. This causes broad separation in the morning and afternoon line segments with brief spike separation when clouds are present.

We have computed these plots for these three days (Figure 6 and Figure 7). Two features stand out in the plots. The first is the rapid speed with which the cloud spikes rise, compared to baseline changes associated with aerosol changes. The second feature is the decreases in radiance during relatively clear moments during cloudy periods. It is also clear that the radiances at 440 nm are much higher than those at 870 nm. This is due to the  $1/\lambda^4$  dependence of Rayleigh scattering.

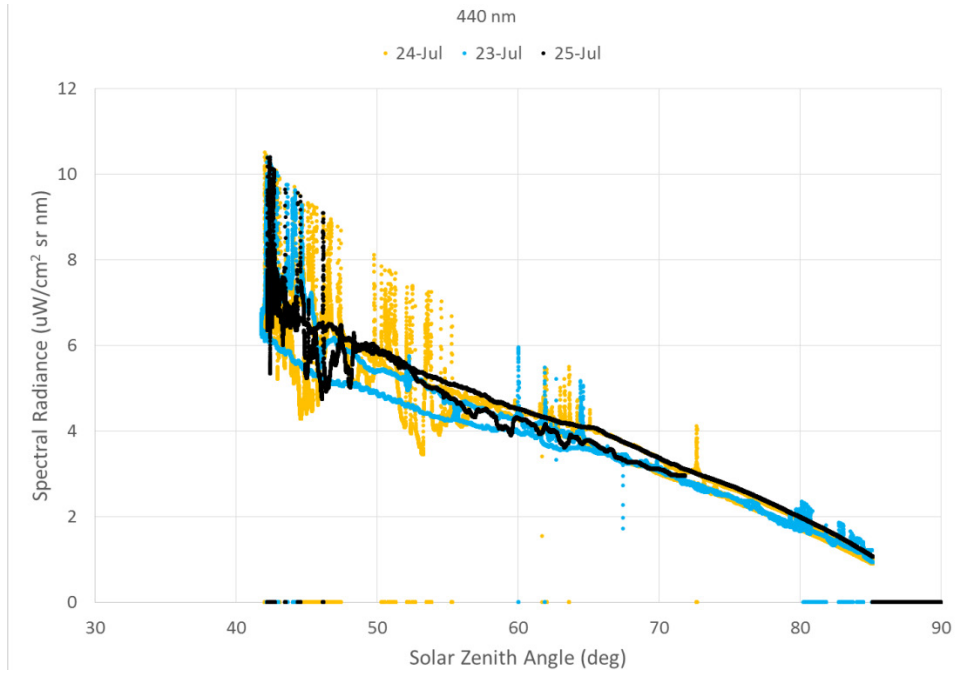


**Figure 6.** Spectral Radiance at 440 nm for 23-25 July 2014 plotted against Solar Zenith Angle.

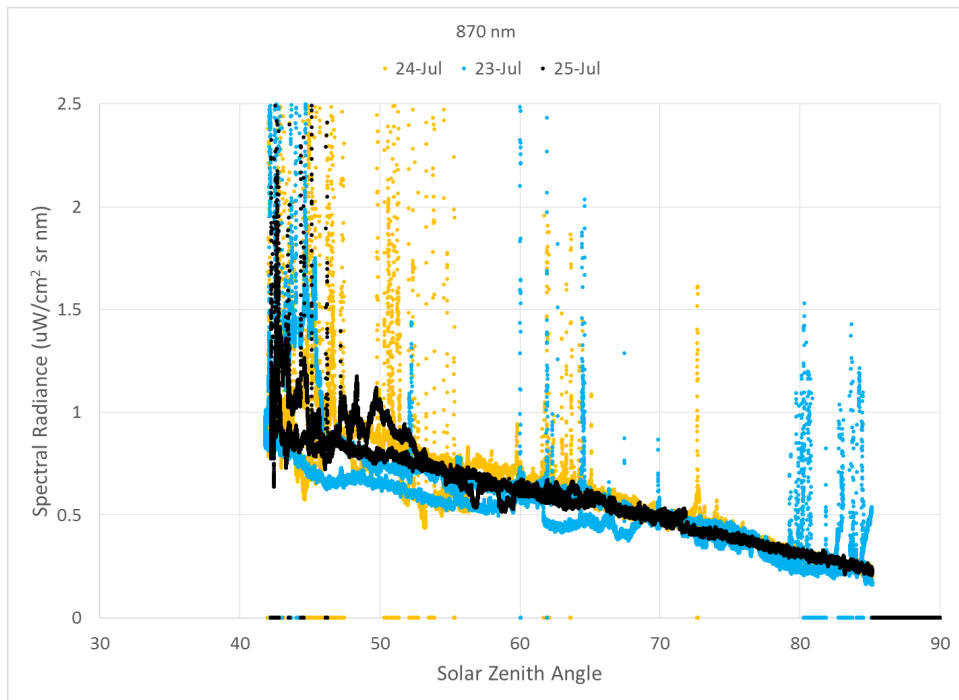


**Figure 7.** Spectral Radiance at 870 nm for 23-25 July 2014 plotted against Solar Zenith Angle.

If we overlay these same plots with the expected radiances for various levels of aerosols, we can get an approximate value of aerosol visibility (Figure 8 and Figure 9). Based on the plots, the aerosol visibility is between 100 and 50 kilometers (km).

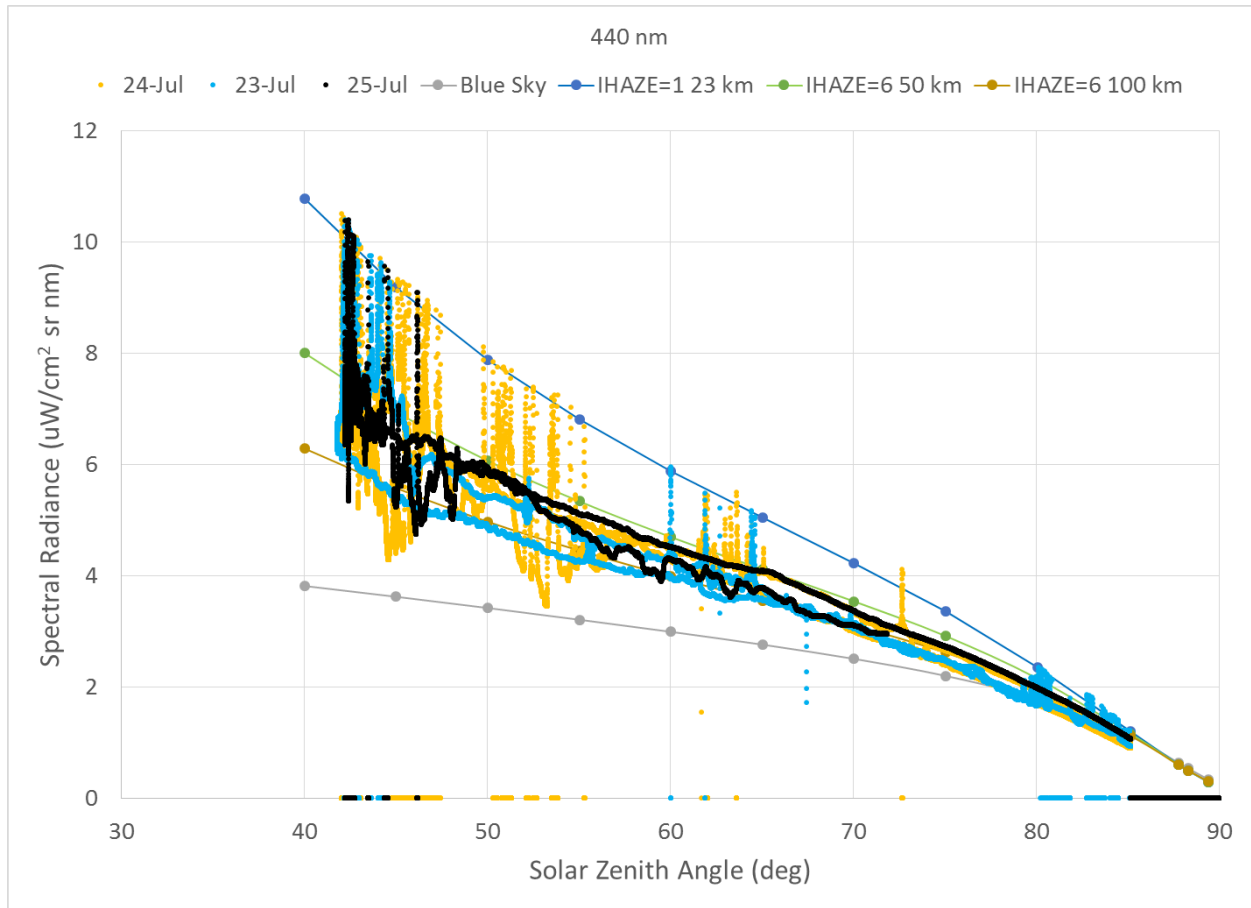


**Figure 8.** Spectral Radiance at 440 nm for 23-25 July 2014 plotted against Solar Zenith Angle overlaid with the expected spectral radiance at 440 nm for four levels of aerosol: no aerosol (gray line), IHAZE=6 at 100 km visibility (mustard line), IHAZE=6 at 50 km visibility (green line) and IHAZE=1 at 23 km visibility (blue line) using MODTRAN® 5.2.

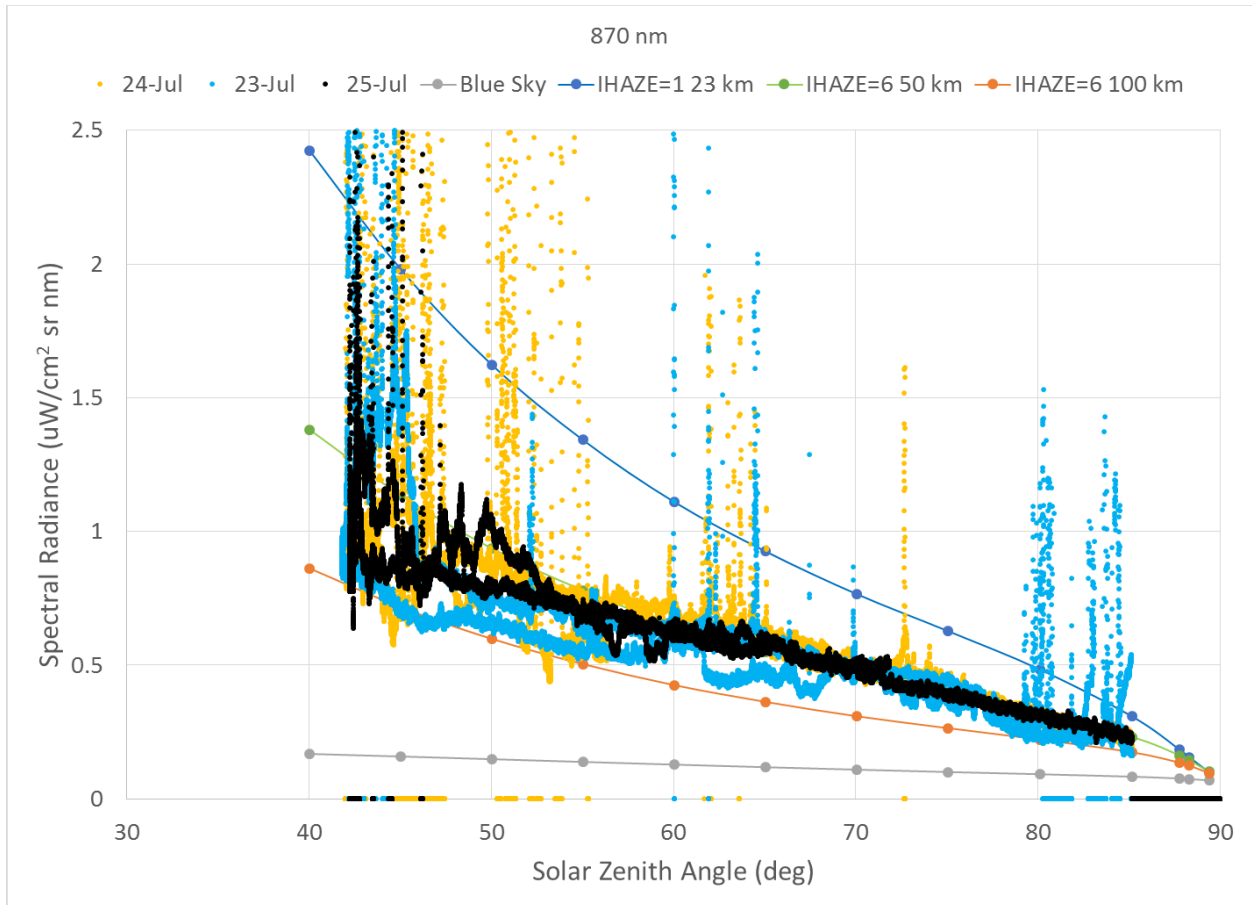


**Figure 9.** Spectral Radiance at 870 nm for 23-25 July 2014 plotted against Solar Zenith Angle overlaid with the expected spectral radiance at 870 nm for four levels of aerosol: no aerosol (gray line), IHAZE=6 at 100 km visibility (mustard line), IHAZE=6 at 50 km visibility (green line) and IHAZE=1 at 23 km visibility (blue line) using MODTRAN® 5.2.

If we examine the behavior around 45 degree solar zenith angle on July 24, we see large decreases in the 440 nm spectral radiances in between passing clouds. This is a little easier to see on an expanded time plot (Figure 10). The levels are so low that they fall significantly below the cloud-free periods before and after the cloudy period. There are two different phenomena that can cause decreases. The first is a decrease in the aerosol; less aerosol means less scattered light. The second is a cloud shadow that is evident in the TSI data from around this time (Figure 11). We are not certain which effect is dominant during this period. We plan to investigate it further by working with some of the data from other instruments.

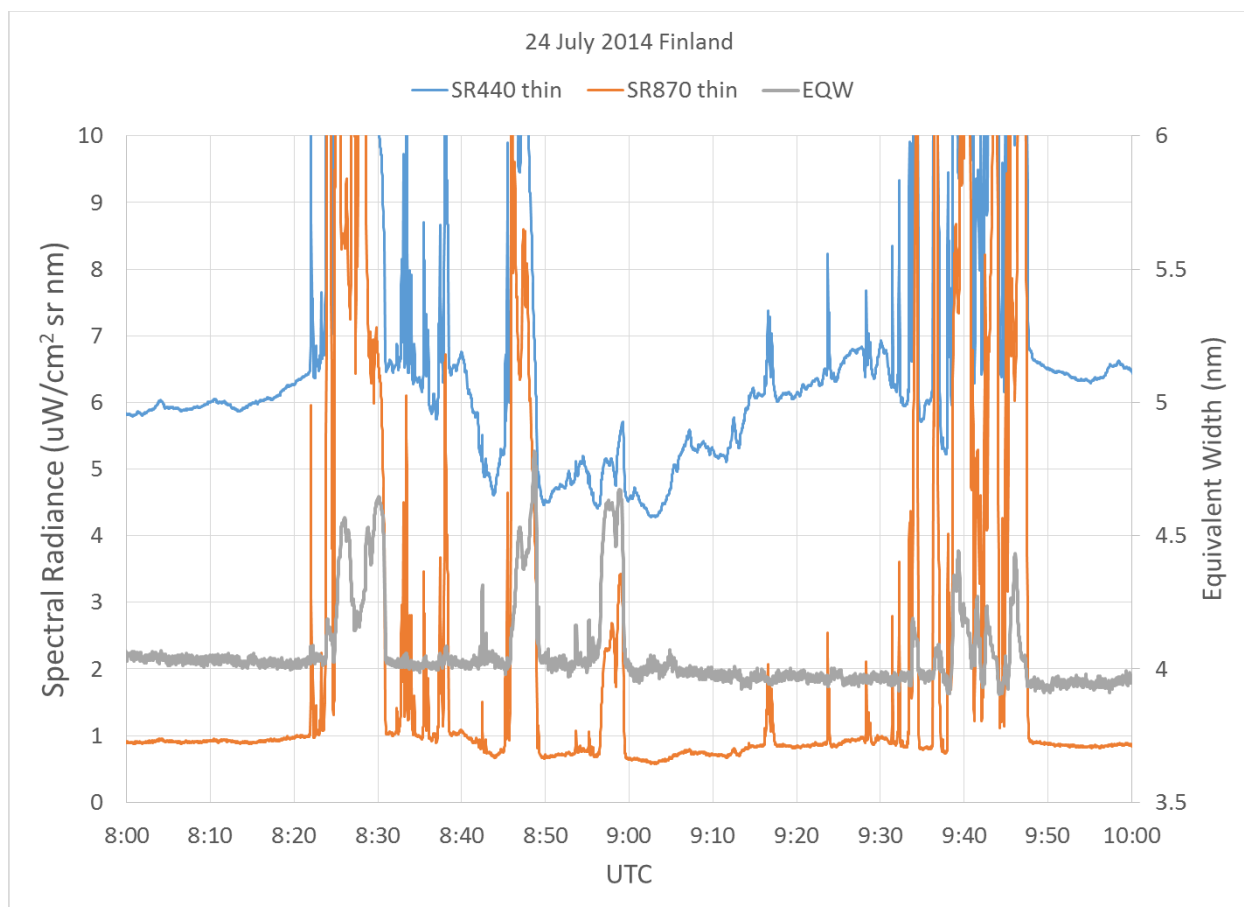


**Figure 10.** Spectral Radiance at 440 and 870 nm (left-hand axis) and the equivalent width of the oxygen A-band (gray curve and right-hand axis) versus time.



**Figure 11.** Cloud shadow from TSI sensor for July 24 2014 9:39 UTC.

## 6.0 TWST ARM Data Archive Description

The CODs produced by TWST have been placed on the ARM Data Archive. The data for each day are contained in a single, comma-separated-values ASCII file. The individual files are named for the date (UTC), e.g., TWSTCOD\_20140716.txt for the data from July 16 2014. The data set includes both raw data and processed data. The raw data consists of one line of data for each collection time. The line starts with the time (UTC), then presents the calibrated spectral radiances of the zenith sky overhead at 440 and 870 nm with an approximate spectral resolution of 2.5 nm, then the equivalent width of the oxygen A-band, followed by a status comment about the cloud optical state, then the solar zenith angle, and finally the COD. There is one line for approximately each second of daylight, less a 5-10 second period every 60 seconds during which a dark spectrum is collected. The units for the spectral radiance is [microwatts/cm<sup>2</sup> sr nm]. The field of view of the sensor is approximately 0.5 degree full angle. The STATUS variable is limited to: “Out of Range” when the solar zenith angle is greater than our lookup table range, “Unknown” when our algorithm uncertainty is too high, “Blue sky” when no clouds are present, “Bluish” when cloud is optically very thin, “Thin” when optically thin, “3D cloud” when the cloud spectral radiance at 440 nm is higher than the highest spectral radiance in our lookup table, and “Thick” when the cloud is optically thick.

The data set is considered complete for the information presented, as described in the abstract. Users are advised to read the rest of the metadata record carefully for additional details. All data collected during periods of questionable operation of the sensor have been trimmed out of the data files. This includes periods during five days (7/17, 7/18, 7/20, 7/21, 7/22) when the sensor baseline drift exceeded nominal thresholds. The data files for these days include the word “trimmed” in the file name to indicate this fact. The condition was corrected at 12:16:27 (UTC) on 22 July, so no data files after this time have been trimmed. In addition, times just after dawn or before sunset are more susceptible to three-dimensional (3D) cloud effects due to the long path length of the solar radiation. Our sensor also has automatic thresholding on the oxygen A-band equivalent width to eliminate times when the value is greater than six. There is also a brief period during each morning, usually around 6:30 UTC, when the window was inspected and cleaned if necessary by onsite staff.

## 7.0 Bibliography

Berk, A, GP Anderson, PK Acharya, and EP Shettle. 2011. “MODTRAN 5.2.1 User’s Manual,” Spectral Sciences, Inc., Burlington, Massachusetts.

Chiu, JC, C-H Huang, A Marshak, I Slutsker, DM Giles, BN Holben, Y Knyazikhin, and WJ Wiscombe. 2010. “Cloud optical depth retrievals from the Aerosol Robotic Network (AERONET) cloud mode observations.” *Journal of Geophysical Research–Atmospheres* 115(D14202), [doi:10.1029/2009JD013121](https://doi.org/10.1029/2009JD013121).

Conant, J and E Niple. 2014. “Using MODTRAN computations in a real-time Cloud Optical Depth sensor.” Presented at the 2014 IEEE Transmission Meeting 35<sup>th</sup> Review of Atmospheric Transmission Models. Albuquerque, New Mexico.

Holben, BN, TF Eck, I Slutsker, D Tanré, JP Buis, A Setzer, E Vermote, JA Reagan, YJ Kaufman, T Nakajima, F Lavenue, I Janowiak, and A Smirnov. 1998. “AERONET—A federated instrument network and data archive for aerosol characterization.” *Remote Sensing of the Environment* 66(1): 1-16, [doi:10.1016/S0034-4257\(98\)0031-5](https://doi.org/10.1016/S0034-4257(98)0031-5).

Niple, E, H Scott, F Iannarilli, J Conant, and S Jones. 2014. Field Evaluation of Real-time Cloud OD Sensor TWST during the DOE-ARM-TCAP Campaign, 2013. U.S. Department of Energy. DOE/SC-ARM-14-016. <https://www.arm.gov/publications/programdocs/doe-sc-arm-14-018.pdf>

## Appendix A

### Daily Summary Plots

This appendix contains daily summary plots of the inputs and outputs from the TWST COD algorithm. The data plotted here is the same as those available from the ARM Data Archive website. The format of the plots is described in the Section V of the report, which is repeated here:

“For each of the days that TWST was deployed in Finland, we have prepared two summary charts that show the inputs and the outputs from the post-processing. The first of the two plots shows the calibrated spectral radiances at 440 (blue line) and 870 (orange line) nm (in units of microwatts/cm<sup>2</sup> sr nm) along with the equivalent width (gray line) of the oxygen A-band (in units of nm) for the entire daylight period. The second plot shows the corresponding optically thin (blue line) and optically thick (orange line) cloud optical depths and the post-processing algorithm’s selection (gray squares) for the final cloud optical depth based on the estimated cloud state (optically thick or optically thin). These final COD values are labelled “RatCOD” in the plot legends.”

